Benha Journal of Applied Sciences (BJAS) **print: ISSN 2356–9751**
Vol. (10) Issue (4) (2025), (89- 100) **online: ISSN 2356–976x**

http://bjas.bu.edu.eg
engineering sciences

Sampling Frequency Offset Estimation in OFDM Systems: A comparative study

Moatasem M.E.Kotb , Maha R.Abdel-Haleem, A.Y.Hassan and Ashraf S.Mohra
EE Dept. Benha faculty of engineering, Benha University, Benha, Egypt.
E-mail: Mutasim.Qutb20@beng.bu.edu.eg

Abstract
This study investigates the impact of Sampling Frequency Offset (SFO) on Orthogonal Frequency Division Multiplexing (OFDM) system performance and proposes novel estimation techniques to enhance accuracy. A comprehensive analysis of SFO-induced degradation, including its effects on Bit Error Rate (BER), is presented, along with an evaluation of existing estimation methods such as the Phase Difference (PD), Correlation-Based (CB), PD-Weighted by Subcarrier Index (PD-WSI), and Hybrid Estimation (H-EST) techniques. To improve estimation precision, we introduce three novel methods: SFOest1, an initial enhanced estimator; SFOest1_p, an optimized version with refined weighting bias factors; and SFOest2, which incorporates an iterative subcarrier weight optimization strategy for superior accuracy. Extensive Monte Carlo simulations demonstrate that SFOest2 consistently achieves the lowest Root Mean Square Error (RMSE) and BER across varying Signal-to-Noise Ratio (SNR) conditions, outperforming existing methods. Comparative BER analysis further validates the effectiveness of the proposed techniques, with SFOest2 exhibiting the strongest robustness. The results highlight the potential of these methods to replace conventional SFO estimation approaches in modern communication systems.

Keywords: Frequency synchronization, SFO estimation, Subcarrier weighting, Data-Aided (DA) techniques, Phase Difference-based SFO estimation, Correlation-based SFO estimation, and Wireless Communication.

I. INTRODUCTION

Orthogonal Frequency Division Multiplexing (OFDM) has become a cornerstone of modern wireless communication systems, renowned for its high spectral efficiency, resilience to multipath fading, and capacity to support elevated data rates. Its widespread adoption spans applications such as wireless broadband, digital broadcasting, and next-generation mobile networks. However, despite these advantages, OFDM is inherently vulnerable to synchronization errors—most notably Sampling Frequency Offset (SFO). SFO stems from discrepancies between the sampling clocks of the transmitter and receiver, often caused by oscillator imperfections, clock drift, or hardware constraints. Unlike Carrier Frequency Offset (CFO), which uniformly affects all subcarriers, SFO introduces a linearly varying phase shift across subcarriers. This disrupts the orthogonality essential to OFDM operation, resulting in Inter-Carrier Interference (ICI) and system degradation [1-2]. Specifically, SFO induces phase rotations that impair symbol detection, causes temporal drift leading to symbol misalignment, and introduces timing errors that compromise sampling accuracy. These effects collectively increase the Bit Error Rate (BER), reduce system reliability, and challenge signal recovery—especially in high-throughput environments [3-5]. To counteract SFO, numerous estimation and compensation strategies have been proposed. Pilot-aided techniques leverage known symbols embedded in the signal for tracking and correction, while data-aided methods utilize reference data for estimation. Additionally, blind techniques infer frequency mismatches by exploiting signal properties without relying on pilots. Despite considerable progress, accurate and robust SFO estimation remains a critical challenge, particularly under dynamic or low Signal-to-Noise Ratio (SNR) conditions [6-7].

The objectives of our research were threefold. First, we investigated the impact of sampling frequency offset on the performance of OFDM systems, with a particular focus on its influence on the BER. Second, we conducted a comprehensive review of existing SFO estimation techniques, identifying key methods that serve as benchmarks. Finally, we introduced a novel estimation approach designed to improve the accuracy and robustness of SFO estimation in OFDM environments.

Key Contributions of This Work:

1. **Comprehensive Analysis of SFO in OFDM** – Investigated the impact of sampling frequency offset on system performance, including its effects on BER.
2. **Evaluation of Existing Estimation Methods** – Analyzed existing SFO estimation techniques such as Phase Difference (PD) method, Correlation-Based (CB) method, Phase Difference Weighted by Subcarrier Index (PD-WSI) method, and Hybrid Estimation (H-EST) method.
3. **Proposal of Novel Estimation Technique** – Introduced a new estimation method, referred to as SFOest1, to enhance SFO estimation accuracy.
4. **Improving the Estimation Precision of SFOest 1** – Developed an optimization framework for the weighting bias factor in SFOest1 to improve estimation precision; the resulting method is referred to as SFOest1_p.
5. **Iterative Weight Optimization in SFOest2** – Implemented a subcarrier weighting strategy, resulting in superior SFO estimation performance; we refer to this method as SFOest2.
6. **Extensive Monte Carlo Simulations** – Conducted performance evaluations under various SNR levels, demonstrating that SFOest2 consistently

achieves the lowest Root Mean Square Error (RMSE) and BER.

7. **Comparative BER Analysis** – Provided a detailed comparison of BER curves, confirming that the proposed methods significantly outperform existing approaches (PD, CB, PD-WSI, and H-EST) in mitigating SFO-induced degradation.
8. **Potential to Replace Existing SFO Estimation Techniques:** Given their superior accuracy, our proposed methods have the potential to replace existing SFO estimation techniques in modern digital communication systems.

The paper is organized as follows: Section II reviews related work, Section III introduces the proposed method, Section IV presents the results along with their analysis, and Section V concludes the paper with final remarks.

II. SURVEY

Previous studies on sampling frequency offset estimation have employed different methods. Fischer et al. [8] proposed a two-stage frequency synchronization strategy for OFDM receivers, aimed at improving the accuracy of frequency offset detection and correction. The first stage, known as frequency acquisition, employs Fast Fourier Transform (FFT)-based power spectral density estimation to detect the frequency pilots of Digital Radio Mondiale (DRM) and identify initial frequency offsets. The second stage, frequency tracking, enhances synchronization by measuring phase increments between successive OFDM symbols and continuously correcting any residual errors. Additionally, the approach compensates for sample rate offsets by analyzing frequency deviations across multiple pilots. While effective, this method requires averaging over multiple symbols to mitigate errors caused by fading and noise. Shim et al. [9] proposed a two-stage synchronization approach to address critical synchronization issues in OFDM-based frequency modulation (FM) broadcasting systems, including timing offset, carrier frequency offset, and sampling frequency offset. The first stage, pre-FFT synchronization, estimates symbol timing using the cyclic prefix (CP) correlation and determines fractional frequency offset by analyzing phase differences between the CP and the useful portion of the OFDM symbol. The second stage, post-FFT synchronization, involves integer frequency offset estimation based on time reference cells and further refines synchronization by tracking residual frequency offset and SFO using gain reference cells. Notably, SFO mitigation in this approach is achieved through a post-FFT technique that relies on phase difference calculations, ensuring more accurate estimation. Shin, Seo, and You [10] analyzed Sampling Frequency Offset estimation in OFDM-based DRM systems by proposing two primary algorithms. Algorithm A estimates SFO by leveraging the phase difference between neighboring Frequency Reference Cells (FRCs), utilizing temporal correlation to enhance accuracy. Algorithm B builds upon this approach by incorporating differential relations among FRC indices, further refining the estimation precision. Additionally, the authors introduced a low-complexity estimation technique that reduces computational demands by modifying the temporal correlation method to rely solely on the first and last noise measurements.

Harish, Chuppala, Rajasekar Mohan, and R. Shashank [11] proposed a method for estimating and correcting sampling frequency offset in OFDM receivers by leveraging the assumed proportional relationship between SFO and carrier frequency offset. Their approach is based on the idea that both the sampling clock and the carrier frequency oscillator in the receiver originate from the same reference source, leading to a mathematical correlation between CFO and SFO. The estimation process begins with determining the CFO using training sequences in the received OFDM frame through autocorrelation techniques. Once the CFO is estimated, the SFO is computed using the proportionality equation $\delta fc/fc=\delta fs/fs$, which allows for a systematic correction of SFO-induced errors. The correction is applied in the frequency domain by incorporating a phase compensation factor in the FFT output, ensuring improved synchronization without requiring complex hardware-based clock recovery mechanisms. While this approach is computationally efficient, its effectiveness depends on the assumption that both oscillators originate from the same reference source, which may not always be valid in practical systems. Jung and Young-Hwan You [12] proposed a robust sampling frequency offset estimation method for OFDM systems operating over frequency-selective fading channels. Their approach consists of two key techniques: temporal correlation and frequential correlation. The temporal correlation method leverages the relationship between received pilot symbols to mitigate the impact of unknown channel responses, thereby reducing the effect of channel variations over time. Additionally, the frequential correlation technique improves accuracy by exploiting the symmetry of pilot subcarriers around the DC carrier, effectively eliminating bias caused by frequency-selective fading. This combined approach enhances the robustness of SFO estimation, making it more resilient to adverse channel conditions. Liu et al. [13] conducted a comprehensive analysis of various synchronization algorithms for OFDM systems, with a particular focus on symbol timing synchronization, carrier frequency synchronization, and sampling clock synchronization. The study evaluates multiple techniques, including the Schmidl & Cox (SCA) algorithm, the Minn algorithm, Pilot-based Carrier Frequency Synchronization, and the Maximum Likelihood (ML) algorithm, to assess their effectiveness in accurately correcting timing and frequency offsets. Furthermore, the paper suggests that sampling frequency offset can be mitigated through interpolation filters, which adjust the sampling instants at the receiver after detection, thereby reducing synchronization errors caused by SFO. Hsiao et al. [14] proposed a clock synchronization technique for OFDM-based communication that focuses on estimating and correcting the sampling frequency offset in the frequency domain. Their method relies on observing the phase rotation across OFDM subcarriers to estimate SFO, offering a computationally efficient approach to synchronization. However, the study lacks a direct performance comparison with other existing SFO

estimation methods, making it difficult to evaluate its relative effectiveness. Additionally, the technique may be sensitive to varying channel conditions, which could impact its robustness in practical implementations. Another limitation is the assumption of a free-running Analog-to-Digital Converter (ADC), which may not align with all hardware configurations, potentially restricting its applicability in real-world OFDM systems. Kumar [15] explored frequency synchronization in frequency-domain Orthogonal Frequency Division Multiplexing with Index Modulation (OFDM-IM)-based Wireless Local Area Network (WLAN) systems, proposing an autocorrelation matrix-based method to estimate frequency offsets. This technique tracks phase distortions, enabling more precise synchronization by compensating for sampling frequency offset when timing drift accumulates over multiple symbols. By leveraging autocorrelation properties, the method enhances synchronization accuracy, potentially improving overall system performance in WLAN environments. Table 1 provides a summary of the previously discussed research.

Table 1 : Survey Summary

Paper / Authors	Problem	Technique	Drawbacks
V. Fischer and A. Kurpiers [8]	Frequency Synchronization	Two-stage frequency synchronization: (1) Frequency acquisition using FFT-based power spectral density estimation, (2) Frequency tracking via phase increment measurements. Sample rate offsets are compensated by analyzing frequency deviations.	Requires averaging over multiple symbols to mitigate errors from noise.
E.-S. Shim, et al.[9]	Synchronization Issues (Timing Offset (TO), CFO, and SFO)	Two-stage approach: Pre-FFT synchronization (symbol timing via CP correlation, Fractional Frequency Offset via phase differences) and Post-FFT synchronization (Integer Frequency Offset estimation, Residual Frequency Offset and SFO tracking using reference cells).	-
W.-J. Shin, J. Seo, and Y.-H. You [10]	Sampling Frequency Offset	Two main algorithms: (A) Phase difference between neighboring FRCs, leveraging temporal correlation; (B) Differential relations among FRC indices for precise estimation. Introduces a low-complexity estimation method that reduces computational burden.	-
H. Chuppala, R. Mohan, and R. Shashank [11]	Sampling Frequency Offset	Uses the proportional relationship between CFO and SFO. First estimates CFO using autocorrelation methods, then computes SFO via a proportionality equation. Corrects SFO-induced error in the frequency domain with phase compensation at the FFT output.	Assumes carrier frequency oscillator and sampling clock oscillator share the same reference source, which may not always be valid.
Y.-A. Jung and Y.-H. You [12]	Sampling Frequency Offset	Uses temporal correlation between received pilot symbols to counteract unknown channel responses and frequency correlation among pilot subcarriers to eliminate bias from frequency-selective fading.	-
M. Liu, et al. [13]	Symbol Timing, Carrier Frequency, and Sampling Clock Synchronization	Compares different synchronization algorithms (Schmidl & Cox, Minn, Pilot-based, Maximum Likelihood). Suggests SFO correction using interpolation filters after detection.	-
C.-Y. Hsiao, et al. [14]	Sampling Clock Offset	Frequency domain SFO estimation via phase rotation across OFDM subcarriers.	Lacks performance comparison with other SFO estimation methods. Potential sensitivity to channel conditions. Assumes a free-running ADC.
N. Kumar [15]	Frequency Synchronization	Uses an autocorrelation matrix-based method to estimate frequency offsets by tracking phase distortions, aiding in SFO compensation.	-

III. PROPOSED METHOD

The proposed method section consists of two subsections. Subsection A focuses on the influence of the SFO on the system performance, while subsection B outlines the methods employed to eliminate this influence.

A. *The impact of SFO on OFDM system*

Let X[k] represent the frequency-domain symbols (modulated data on subcarriers), where k=0,1,…,N−1 and N is the number of subcarriers. The time-domain signal x[n] is obtained as:

$$x[n] = \frac{1}{N}\sum_{k=0}^{N-1} X[k]e^{j2\pi kn/N} \quad , \quad n = 0,1,\ldots..,N-1 \tag{1}$$

At the receiver, the received signal y[n] is affected by the SFO. If the receiver's sampling frequency fs' differs from the transmitter's sampling frequency fs by Δfs = fs' - fs, the received signal in the time domain can be expressed as:

$$y[n] = x\left(n.\frac{fs}{fs'}\right)e^{j2\pi\epsilon n/N} + w[n] \tag{2}$$

where ε = Δfs/fs is the normalized sampling frequency offset, and w[n] represents additive noise.

In the frequency domain at the receiver, the frequency-domain symbols are recovered as:

$$Y[k] = \sum_{n=0}^{N-1} y[n]e^{-j2\pi kn/N} \tag{3}$$

Substituting y[n] from the time-domain representation:

$$Y[k] = \sum_{n=0}^{N-1}\left(x\left(n.\frac{fs}{fs'}\right)e^{j2\pi\epsilon n/N} + w[n]\right)e^{-j2\pi kn/N} \tag{4}$$

This can be rewritten as:

$$Y[k] = \sum_{n=0}^{N-1} x\left(n.\frac{fs}{fs'}\right)e^{j2\pi\epsilon n/N}\,e^{-j2\pi kn/N} + W[k] \tag{5}$$

where W[k]=FFT{w[n]} is the noise in the frequency domain.

The SFO manifests in the frequency domain through two key effects. First, it causes subcarrier leakage, also known as ICI, which disrupts the orthogonality between subcarriers. This can be mathematically expressed as:

$$Y[k] = X[k].H[k].sinc(\pi\epsilon) + \sum_{m\neq k} X[m].H[m].sinc\big(\pi(\epsilon+m-k)\big) + W[k] \tag{6}$$

Here, H[k] represents the channel frequency response, and the sinc function captures the interference from neighboring subcarriers. Second, SFO introduces a phase rotation that grows linearly with the subcarrier index k:

$$\phi[k] = 2\pi\epsilon.\frac{k}{N} \tag{7}$$

This phase rotation must be accurately compensated to ensure proper demodulation of the received signal. Both effects degrade system performance and highlight the importance of SFO estimation and correction in OFDM systems. The following figure illustrates the simulation of how SFO affects the performance of 16QAM-OFDM system.

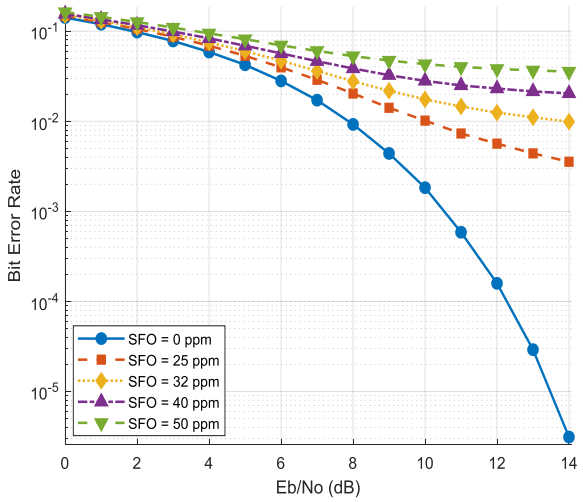

Fig. 1: Impact of SFO on BER of a 16QAM-OFDM system

The perfectly synchronized case (SFO = 0 ppm) shows optimal BER, while increasing SFO introduces inter-carrier interference, degrading performance and causing BER floors at higher offsets.

B. *The methods employed to eliminate the SFO*

This subsection is organized into six parts: subsections (B.1) to (B.4) present four benchmark methods for SFO estimation, while subsections (B.5) and (B.6) describe the proposed methods.

B.1. Phase Difference (PD) Method

This method, derived from the SFO estimation approach in [8], estimates the SFO by analyzing phase shifts between subcarriers in the received frequency-domain signal. Since SFO causes phase rotations proportional to subcarrier indices, a reference subcarrier is used to provide a stable baseline. The relative phase differences between the subcarriers are then computed to estimate the sampling frequency offset, with the reference subcarrier allowing phase differences to be measured without the influence of its inherent phase shift. The phase difference between subcarrier m and the reference subcarrier ref is expressed as:

$$\phi_m = \angle Y[m] - \angle Y[ref] \tag{8}$$

Where $\angle Y[m]$ is the phase of received symbol at subcarrier m.

The estimated SFO is then computed as:

$$\hat{\epsilon}_1 = \frac{1}{2\pi N_c} \sum_{\substack{m=2 \\ m \neq ref}}^{N_c} \frac{\phi_m}{m - ref} \quad (9)$$

where N_c is the total number of subcarriers.
For improved estimation accuracy, this process is modified by weighting scheme.

B.2. Correlation-Based (CB) Method

In contrast to the reference-subcarrier method, which computes phase differences relative to a fixed subcarrier, the correlation-based approach estimates SFO by averaging phase differences between adjacent subcarriers across OFDM symbols. This avoids the need to select a specific reference and reduces the risk of phase wrapping, as the phase differences between neighboring subcarriers tend to be small and stable.

The phase correlation between adjacent subcarriers is given by:

$$\phi_m = \angle(Y[m]Y^*[m-1]) \quad (10)$$

Where $Y^*[m-1]$ is the complex conjugate of $Y[m-1]$, and ϕ_m is the phase difference between adjacent subcarriers

Averaging over all subcarriers gives:

$$\hat{\epsilon}_2 = \frac{1}{2\pi N_c} \cdot \frac{1}{N_c - 3} \sum_{m=3}^{N_c} \phi_m \quad (11)$$

Where $\hat{\epsilon}_2$is the estimated SFO.

B.3. Phase Difference Weighted by Subcarrier Index (PD-WSI) method

This method, derived from the SFO estimation approach in [12, 16, 17], estimates the SFO by analyzing the phase difference between consecutive OFDM symbols. Instead of using a simple phase difference, it estimates the SFO frequency-wise, then weights the phase estimates based on the subcarrier index and averages them over subcarriers. This weighting accounts for the fact that some subcarriers, when weighted differently, contribute to a more accurate estimation of the SFO due to varying amounts of phase rotation. The estimation process is described as follows:

$$\Delta\theta_l[m] = \angle\left(\frac{Y_l[m+1]}{Y_l[m]}\right) \quad (12)$$

$$\Lambda_c = \sum_{l=-\frac{N_c}{2}}^{\frac{N_c}{2}-1} l. \frac{1}{N-1} \sum_{m=1}^{N-1} \Delta\theta_l[m]$$

$$\hat{\epsilon}_3 = \Lambda_c * S_c$$

Where $Y_l[m]$ is the received OFDM symbol in frequency domain at subcarrier l, symbol m, $\Delta\theta_l[m]$ is the phase difference between consecutive symbols at subcarrier l, Λ_c is the weighted sum of phase differences, S_c is scaling factor, and $\hat{\epsilon}_3$ is the estimated SFO.

B.4. Hybrid Estimation (H-EST) Method

The Hybrid SFO Estimation technique, derived from the SFO estimation approach in [12], combines the previous method with intra-symbol phase observations in a dual forward and reverse approach. This dual approach captures both the forward and reverse phase relationships, improving the accuracy of the SFO estimate by mitigating potential phase errors and enhancing robustness to noise and channel distortions. The SFO estimation is given by:

$$\Lambda_P = \sum_{l=-\frac{N_c}{2}}^{\frac{N_c}{2}-1} \sum_{m=1}^{N-1} \left(\angle\left(\frac{Y_l[m+1]}{Y_l[m]}\right) + k_l . \angle\left(\frac{Y_l[m+1]}{Y_l[m]}\right)\right) \quad (13)$$

$$\hat{\epsilon}_4 = \Lambda_P * S_P$$

Where k_l is the frequency bin index for subcarrier l, Λ_P is the combined phase difference, S_P is scaling factor, and $\hat{\epsilon}_4$ is the estimated SFO.

B.5. Proposed Method 1 (SFOest1) and Its Optimized Weighting Bias Factor Version (SFOest1_p)

Our first method estimates the SFO by analyzing phase differences between adjacent OFDM subcarriers across consecutive symbols. Unlike conventional techniques, our approach employs a dual-dimensional analysis of phase ratios—in a distinct manner. This enhances robustness by explicitly accounting for ICI and applies a specialized weighting process to improve estimation accuracy. A normalization factor ensures correct scaling, and the final SFO estimate is obtained by averaging the results. The following equations provide a **detailed** derivation of our proposed method:

The OFDM signal at the transmitter output is given by:

$$x(n) = \frac{1}{N} \sum_{k=0}^{N-1} X(k) e^{j\frac{2\pi}{N}kn} \quad (14)$$

Where N is the number of subcarriers, k is the subcarrier index and n is the sample time index.

The received OFDM signal is expressed as:

$$\dot{x}(n) = x(n) e^{j\frac{2\pi}{N}k_0 n} = \frac{1}{N} \sum_{k=0}^{N-1} X(k) e^{j\frac{2\pi}{N}(k-k_0)n} \quad (15)$$

Where k_0 is the error due to the CFO.

The received OFDM signal, after sampling at the input, is:

$$r(n) = \dot{x}((1+\alpha)n) = \frac{1}{N} \sum_{k=0}^{N-1} X(k) e^{j\frac{2\pi}{N}(k-k_0)(1+\alpha)n} \quad (16)$$

Where α is the SFO.

Let β=1+α, then:

$$r(n) = \frac{1}{N} \sum_{k=0}^{N-1} X(k) e^{j\frac{2\pi n}{N}\beta(k-k_0)} \quad (17)$$

The FFT representation of subcarrier *j* at the receiver is:

$$R(j) = \sum_{n=0}^{N-1} r(n) e^{j\frac{2\pi}{N}jn} \tag{18}$$

Substituting equation (17) into equation (18) yields:

$$R(j) = \frac{1}{N}\sum_{n=0}^{N-1}\sum_{k=0}^{N-1} X(k) e^{j\frac{2\pi n}{N}\beta(k-k_0)} . e^{-j\frac{2\pi}{N}jn} \tag{19}$$

$$R(j) = \frac{1}{N}\dot{X}(j)\sum_{n=0}^{N-1} e^{j\frac{2\pi n}{N}(\beta j - \beta k_0 - j)}$$

Where $\dot{X}(j)$ is the distorted X at subcarrier j.

Let $\theta_j = \beta j - \beta k_0 - j$,then:

$$R(j) = \frac{1}{N}\dot{X}(j)\sum_{n=0}^{N-1} e^{j\frac{2\pi n}{N}\theta_j} \tag{20}$$

Since $\sum_{n=0}^{N-1} e^{j\frac{2\pi n}{N}\theta_j}$ forms a finite geometric series, $R(j)$ can be can be reformulated as:

$$R(j) = \frac{1}{N}\dot{X}(j).\frac{e^{j2\pi\theta_j} - 1}{e^{j\frac{2\pi}{N}\theta_j} - 1} \tag{21}$$

$$R(j) = \frac{1}{N}\dot{X}(j) e^{j\left(\pi - \frac{\pi}{N}\right)\theta_j} . N\, Sinc\left(\pi\theta_j\right)$$

At time index N_0, $R_{N_0}(j)$ takes the form:

$$\dot{x}(n - N_0) = \frac{1}{N}\sum_{k=0}^{N-1} X(k) e^{j\frac{2\pi}{N}(k-k_0)(n-N_0)} \tag{22}$$

$$r(n - N_0) = \dot{x}(\beta(n - N_0)) = \frac{1}{N}\sum_{k=0}^{N-1} X(k) e^{j\frac{2\pi}{N}\beta(k-k_0)(n-N_0)}$$

$$R_{N_0}(j) = \sum_{n=0}^{N-1} r(n + N_0) e^{-j\frac{2\pi}{N}j(n-N_0)}$$

$$= \frac{1}{N}\dot{X}(j) e^{j\left(\pi - \frac{\pi}{N}\right)\theta_j} . N\, Sinc\left(\pi\theta_j\right). e^{j\frac{2\pi}{N}(\beta j - \beta k_0 - j)N_0}$$

The estimation of the SFO is carried out as:

$$angle\left(\frac{R_{N_0}(j)}{R(j)}\right) = +\frac{2\pi}{N}(\beta j - \beta k_0 - j)N_0 \tag{23}$$

$$angle\left(\frac{R_{N_0}(j+1)}{R(j+1)}\right) = +\frac{2\pi}{N}(\beta j + \beta - \beta k_0 - j - 1)N_0$$

$$angle\left(\frac{R_{N_0}(j+1)}{R(j+1)}\right) - angle\left(\frac{R_{N_0}(j)}{R(j)}\right) = +\frac{2\pi}{N}N_0[\beta - 1] = \Delta$$

Reapplying the substitution β=1+α, we get:

$$[1 + \alpha - 1] = \frac{\Delta N}{2\pi N_0} \tag{24}$$

$$\alpha = \frac{\Delta N}{2\pi N_0}$$

This approach is iterated for N OFDM subcarriers and M OFDM symbols. The phase difference, denoted as $\Delta\phi_{j,q}$, represents the shift between successive subcarriers and symbols, where j and q correspond to the subcarrier and symbol (time) indices used for its computation. A weighting process is applied to refine the estimation. The phase estimates are weighted based on the subcarrier index as:

$$w_j = \frac{(1-p)N^{-1} + p.\frac{1}{2}\left(1 - \cos\left(\frac{2\pi j}{N-1}\right)\right) + (1-p)N^{-1} + p.\frac{1}{2}\left(1 - \cos\left(\frac{2\pi(N-j+1)}{N-1}\right)\right)}{2\sum_{j=1}^{N} w_j} \tag{25}$$

Where w_j is the weight associated with subcarrier j, and p is the weighting bias factor (0≤p≤1). P value is arbitrary selected (fixed) for SFOest 1 method.

The refined SFO estimation is given by:

$$\hat{\epsilon}_5 = S_f \sum_{j=1}^{N-1}\sum_{q=1}^{M-1} w_j . \frac{\Delta\phi_{j,q}}{2\pi N} \tag{26}$$

where S_f is scaling factor.

For **SFOest 1_p**, the weighting bias factor is optimized in the following 5 steps:

Step 1: Objective Function Definition

The objective function J(p) is defined as:

$$J(p) = |f(w(p), R) - \epsilon_{true}| \ , p \in [0,1] \tag{27}$$

Where $f(w(p), R)$ is the SFO estimator function (as defined in Equation 26) for the received signal R in the frequency domain, and ϵ_{true} is the true SFO value.

Step 2: Weight Vector Construction and SFO Estimation

Based on equation (25), the subcarrier weights are computed as a convex combination of uniform and Hann window weights, given by:

$$w(p) = \frac{(1-p)u + pc + \mathbb{R}\left((1-p)u + pc\right)}{2.\|(1-p)u + pc\|_1} \tag{28}$$

Where $u = \frac{1}{N}$ is the uniform weight vector, c is the Hann window vector with $c_j = 0.5\left(1 - \cos\left(\frac{2\pi j}{N-1}\right)\right)$, $\mathbb{R}$ is the vector reversal operator, and $\|\,.\,\|_1$ is the L1-norm.

After the construction of the weight vector the SFO is estimated.

Step 3: Gaussian Process (GP) Modeling

Model the objective function J(p) as a Gaussian Process (GP):

$$J(p) \sim \mathcal{GP}(0, k(p, \acute{p})) \tag{29}$$

With kernel

$$k(p, \acute{p}) = \sigma_f^2\, exp\left(-\frac{(p, \acute{p})^2}{2\ell^2}\right) \tag{30}$$

Where σ_f^2 is the signal variance hyperparameter, and ℓ is the length-scale hyperparameter.

Step 4: Bayesian Loop

For t=1 to n, the following steps are performed:

1. **GP Posterior Update**:
   Given observations
   $\mathcal{D}_{1:t-1} = \{p_i, J(p_i)\}_{i=1}^{t-1}$,
   compute [18,19,20,21]:

$$\mu_t(p) = k_t(p)^T(K_t + \sigma_n^2 I)^{-1} J_{1:t-1} \quad (31)$$
$$\sigma_t^2(p) = k(p,p) - k_t(p)^T(K_t + \sigma_n^2 I)^{-1} k_t(p)$$

2. **Select Next p_t:**
   Maximize Expected Improvement (EI):

$$p_t = \arg\max_{p\in[0,1]} EI(p) \quad (32)$$

Where:

$$EI(p) = (\Delta J_{min} - \mu_t(p))\Phi(Z) + \sigma_t(p)\phi(Z), \quad Z = \frac{\Delta J_{min} - \mu_t(p)}{\sigma_t(p)}$$

3. **Evaluate $J(p_t)$:**
   Compute $w(p_t)$.
   Estimate $\epsilon_{est} = f(w(p_t), R)$.
   Record $J(p_t) = |\epsilon_{est} - \epsilon_{true}|$

Where ΔJ_{min} is the best observed objective value, Φ is the standard normal cumulative distribution function, and ϕ is the standard normal probability density function.

Step 5: p_{opt} Identification

After n evaluations, the GP identifies p_{opt} as the weighting bias factor with the smallest J(p):

$$p_{opt} = \arg\min J(p) \ , p \in [p_1, p_2, \dots\dots, p_n] \quad (33)$$

This process is iterated several times for several SFO values and the optimized weights (using the optimized p) are recorded then the average is taken.

B.6. Proposed Method 2 (SFOest2)

The proposed Method 2 is a modification of Method 1, as both analyze the phase differences between adjacent OFDM subcarriers across consecutive symbols, as discussed in equations (14) to (24). However, SFOest 2 introduces a modified weighting approach, where the weights are optimized through the following steps:

Step1: Initial Weight Calculation (w1) and Objective Function Definition

The initial start of finding the optimum weights is given by:

$$w_1 = \frac{(1-p_0)u + p_0 c}{\|(1-p_0)u + p_0 c\|_1} \quad (34)$$

where p_0 is the initial weighting bias factor.

The objective function J(w) is defined as:

$$J(w) = |f(w,R) - \epsilon_{true}| \quad (35)$$

Where $f(w,R)$ is the SFO estimator function (as defined in Equation 26) for the received signal R in the frequency domain, and ϵ_{true} is the true SFO value.

Step2: Constraints Setup & finding the optimum weights

1. **First setting the constrains as follows:**

$$\sum_{j=1}^{N} w_j = 1\,, \qquad w_j = w_{N-J+1}\,, \quad 0 \le w_j \le 1 \quad (36)$$

2. **Quadratic Approximation:**

At iteration k, approximate the Lagrangian:

$$\mathcal{L}(w,\lambda) \approx \frac{1}{2} d^T H_k d + \nabla J(w_k)^T d + \lambda^T (A_{eq} d) \quad (37)$$

where H_k is the Hessian matrix, and ∇J is the Gradient of the objective.

3. **QP Subproblem:**

Solve for search direction d_k [22-23]:

$$\min_d \frac{1}{2} d^T H_k d + \nabla J(w_k)^T d \quad s.t. \quad A_{eq} d = 0 \quad (38)$$

4. **Line Search:**

Update weights:

$$w_{k+1} = w_k + \alpha_k d_k \quad (39)$$

where α_k ensures $J(w_{k+1}) < J(w_k)$, d_k is the search direction from QP subproblem.

This process is iterated several times for several SFO values and the optimized weights are recorded then the average is taken.

IV. Results and Discussion

The implementation is carried out in MATLAB, and the results are organized into two subsections. Subsection A describes the evaluation method used to test all SFO estimation techniques, while subsection B presents and compares the estimation results, highlighting the performance of each method under identical conditions.

A. Evaluation method

The evaluation of all methods is carried out using the Monte Carlo Testing Procedure, with BER curves also employed to compare their performance. The following outlines the Monte Carlo Testing Procedure utilized:

Step 1: Monte Carlo Simulation Setup

The number of Monte Carlo iterations is defined as:

M = 10,000

RMSE accumulators for each SFO estimation method are initialized as:

$$\sum RMSE_m = 0 \quad (40)$$

$m \in \{PD, CB, PD-WSI, H-EST, SFOest1, SFOest1_{\_p}, and\ SFOest2\}$

Step 2: Signal Generation

For each iteration i = 1, 2, ..., M:

1. Random SFO Selection

A true SFO value $\epsilon^{(i)}$ is randomly chosen from a predefined range:

$$\epsilon^{(i)} \sim P(\epsilon) \quad (41)$$

where $P(\epsilon)$ represents the probability distribution (discrete uniform distribution) over the selected range.

2. SFO-Affected Signal Generation

The generated OFDM signal is affected by the selected SFO, and the received signal is then converted to the frequency domain.

Step 3: SFO Estimation

SFO estimation is then conducted for each method m, resulting in the predicted SFO $\epsilon_m^{(i)}$.

Step 4: RMSE Calculation

1. **RMSE Accumulation**

For each method m, the RMSE accumulation is given by:

$$\sum RMSE_m = \sum_{i=1}^{M} (\epsilon^{(i)} - \hat{\epsilon}_m^{(i)})^2 \quad (42)$$

2. Final RMSE Computation

After all iterations, the final RMSE for each method is computed as [24-25]:

$$\sum RMSE_m = \sqrt{\frac{1}{M} \sum_{i=1}^{M} (\epsilon^{(i)} - \hat{\epsilon}_m^{(i)})^2} \quad (43)$$

B. Sampling frequency offset estimation results

In this subsection, we present the results of the SFO estimation for all methods. We begin with the optimization results of parameter 'p' for the SFOest1_p method in subsection B.1. This is followed by the results for determining the optimal weights 'w' in the SFOest2 method, presented in subsection B.2. In subsection B.3, we provide the Monte Carlo simulation results, where all methods are evaluated under identical conditions. Finally, subsection B.4 offers a comparative analysis of the BER curves for each method.

B.1. Optimization of Parameter 'p' for SFOest1_p results

The relationship between the parameter 'p' and the estimated objective function during the optimization process in the SFOest 1_p method is illustrated in figure 2. The model approximates the true objective function based on observed evaluations, where each point represents the function's output for a specific 'p' value. The model's uncertainty grows between evaluated points, reflecting its confidence in predicting unexplored 'p' ranges. The next point to evaluate is strategically chosen where the model predicts a potential improvement in the objective function—often where low predicted values and high uncertainty intersect. The current best estimate (Red asterisk) indicates the optimal 'p' value found so far, minimizing the estimated objective function. By iteratively updating the model with new evaluations, this approach efficiently navigates the p-space to locate the global optimum.

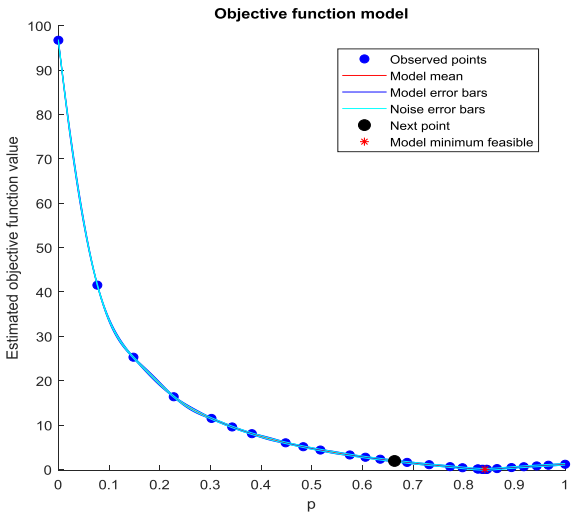

Fig. 2: Parameter 'p' vs. Estimated Objective Function in SFOest1_p

The relationship between the minimum objective value achieved and the cumulative number of function evaluations during an optimization process is illustrated in figure 3. The **min observed objective** plots the best actual function value found so far at each evaluation step, showing how the algorithm progressively discovers better solutions. This curve decreases monotonically, with steeper drops indicating significant improvements and plateaus suggesting temporary local optima. The **estimated min objective** reflects the optimization model's prediction of the minimum value, which may be more optimistic than actual observations early in the process when data is limited (~ evaluations less than 10).

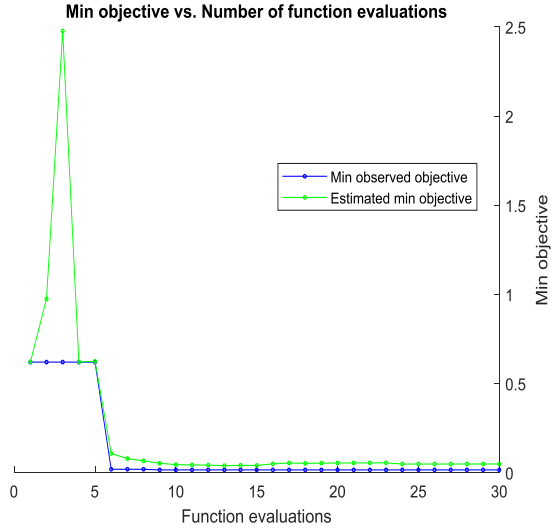

Fig. 3: Minimum Objective Value vs. Cumulative Function Evaluations

As evaluations increase, the gap between observed and estimated minima narrows, demonstrating the model's improving accuracy. The convergence of these curves at around 30 evaluations suggests the algorithm has found a near-optimal solution. The plot's key insight is the trade-off between evaluation count and solution quality - early evaluations yield rapid improvements, while later ones

provide diminishing returns as the optimization refines its solution.

B.2. Optimal Weight Determination for SFOest2 results

The iterative weight optimization process in SFOest2 is illustrated in Figure 4, highlighting the evolution of subcarrier weights through successive computation cycles. Weight values are adjusted through successive iterations, transitioning from initially clustered values to a final differentiated distribution. The plot captures the method's systematic refinement from uniform starting weights to an optimized pattern, demonstrating its targeted compensation approach. The progression demonstrates how the algorithm strategically prioritizes specific subcarriers while attenuating others, optimizing the SFO estimation for maximum accuracy.

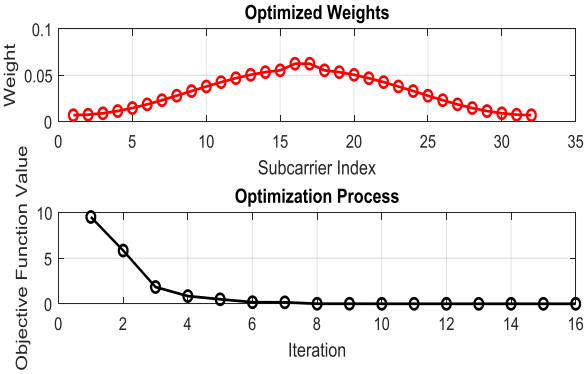

Fig. 4: Iterative Weight Optimization in SFOest2

B.3. Monte Carlo Simulation Results

Monte Carlo simulation results demonstrate the RMSE performance of the methods—PD, CB, PD-WSI, H-EST, SFOest1, SFOest1_p, and SFOest2—across a range of SNR levels. In each simulation, 1,000 OFDM symbols are transmitted over 32 subcarriers, with one SFO estimation performed per 1,000 symbols. A total of 1,000 estimations are conducted, each corresponding to a unique SFO value between 0 and 100 ppm. All methods are tested under identical conditions, using the same fixed number of pilot symbols, and the final RMSE is calculated using Equation (43). Among the tested approaches, SFOest2 consistently achieves the lowest RMSE, particularly at low SNRs, where it significantly outperforms PD, CB, and others. The enhanced SFOest1_p variant also shows strong performance, offering noticeable improvements over SFOest1. In contrast, the remaining methods yield higher estimation errors, especially at SNR values of 15 dB or lower.

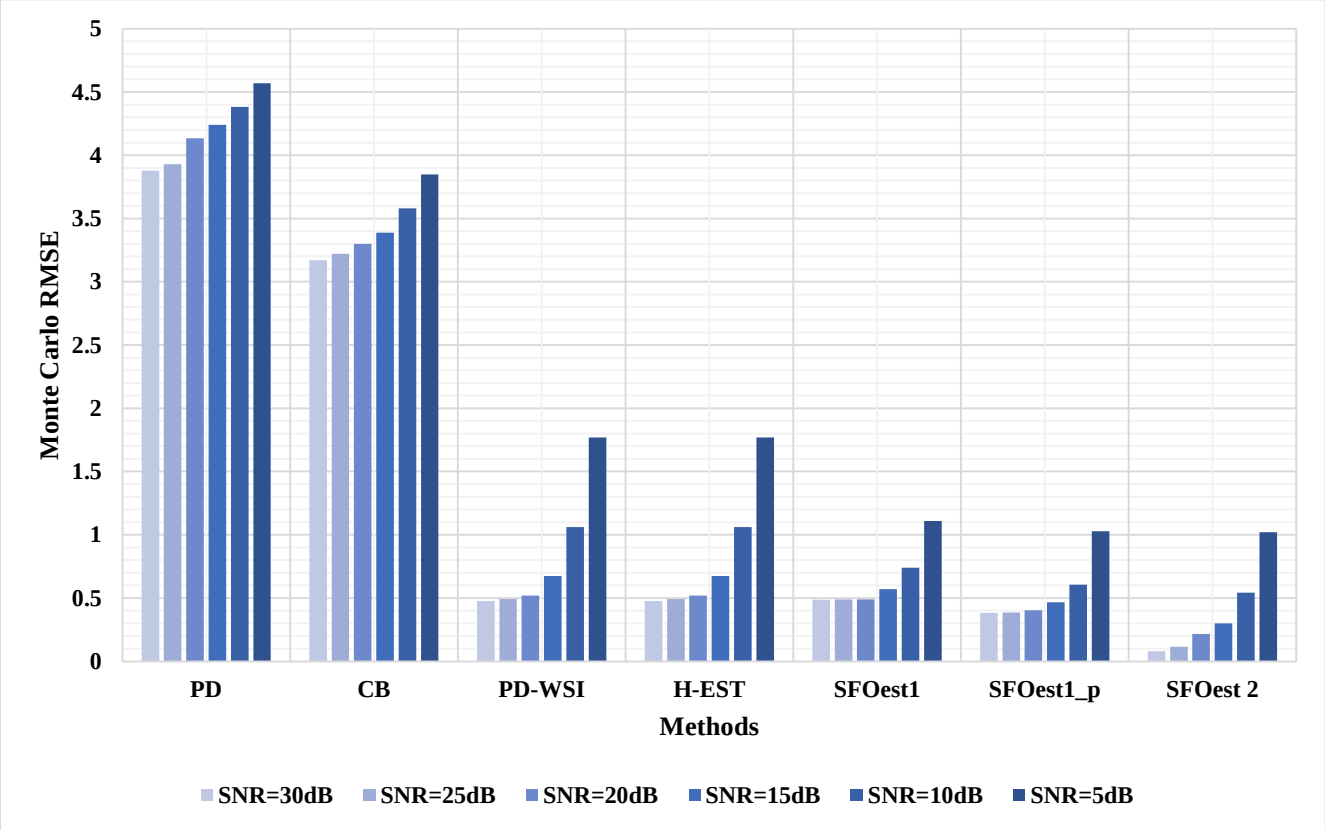

Fig. 5: Monte Carlo Simulation of RMSE Performance Across Methods at Different SNR Levels

B.4. BER Performance Comparison

To assess the effectiveness of various SFO techniques, BER performance was evaluated at two SNR levels: approximately 5 dB and 10 dB. At both SNR points, the presence of high-BER outliers—specifically PD and CB—distorts the BER scale, making it difficult to distinguish the finer differences among the more effective methods. To address this, additional zoomed-in plots were generated to provide clearer insight into the relative performance of the remaining approaches. At 5 dB, the full-range BER plot reveals PD and CB performing poorly, dominating the upper BER range. However, the zoomed-in view exposes the performance gains of intermediate methods like PD-WSI and H-EST, which reduce BER to more acceptable levels. Most notably, the proposed SFOest techniques—SFOest1, SFOest1_p, and SFOest2—achieve significantly lower BERs, with SFOest2 demonstrating the most substantial improvement. This advantage is even more pronounced at 10 dB. While PD and CB remain the weakest performers, the gap between methods becomes clearer. PD-WSI and H-EST show modest improvement, yet they are decisively outperformed by the SFOest variants. Once again, SFOest2 emerges as the most effective method, offering the lowest BER across all test scenarios.

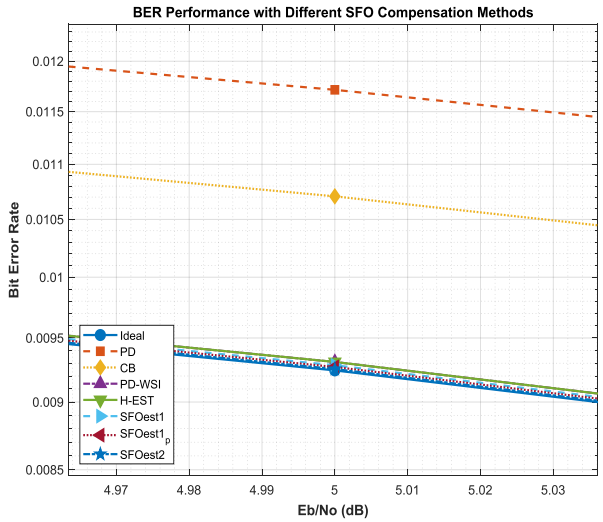

Fig. 6: BER performance of the SFO methods at SNR ~5 dB

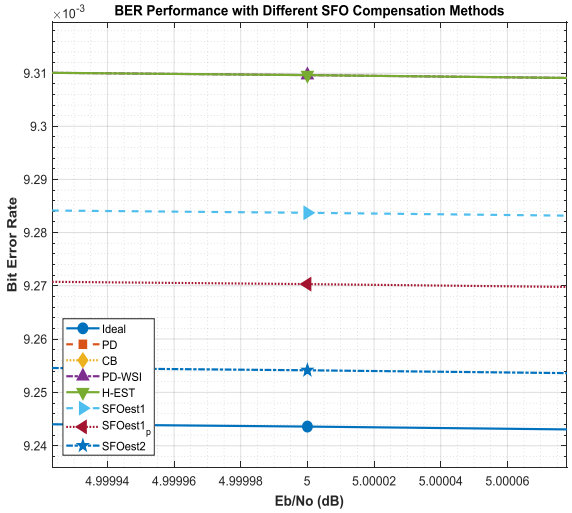

Fig. 7: BER performance of the SFO methods at SNR ~5 dB (zoomed-in view)

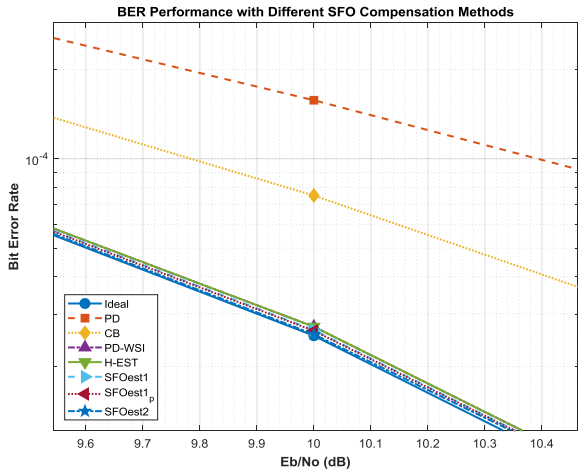

Fig. 8: BER performance of the SFO methods at SNR ~10 dB

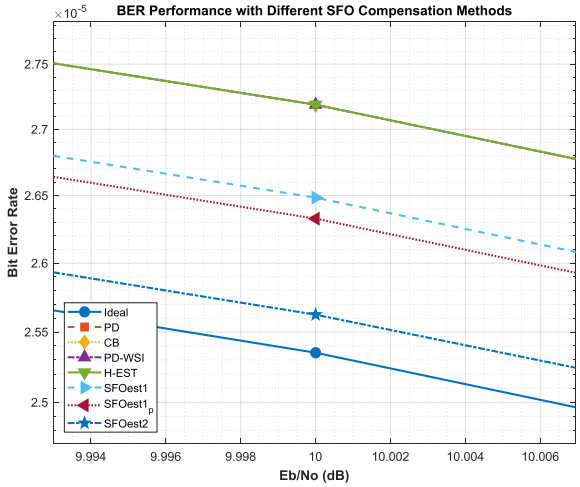

Fig.9: BER performance of the SFO methods at SNR ~10 dB (zoomed-in view)

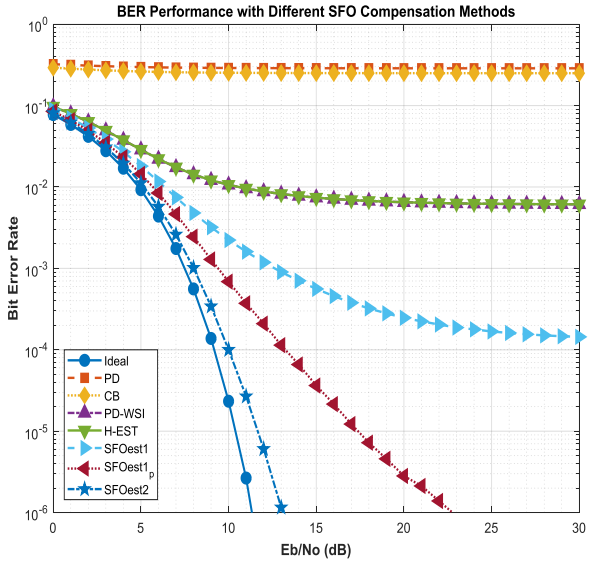

Fig. 10: Evaluation of BER Performance for SFO Methods at Varying Eb/No Values, Emphasizing Residual SFO Effects

Figure 10 compares the BER performance of the SFO methods across increasing Eb/No (dB) values. In this evaluation, a single estimation and compensation process is applied to the transmission of 10,000 OFDM symbols, thereby highlighting the residual SFO accumulation effect on the BER performance of each method. The figure consolidates the trends observed in Figures 6 through 9, providing a clear and comprehensive summary. Overall, the results demonstrate that the proposed methods (SFOest1, SFOest1_p, and SFOest2) consistently outperform the other methods (PD, CB, PD-WSI, and H-EST), with SFOest2 proving to be the most effective in reducing BER.

V. Conclusion

This study investigated the impact of sampling frequency offset on OFDM system performance, analyzed existing estimation methods, and proposed novel estimation techniques to enhance accuracy. Through extensive simulations, we evaluated the proposed methods—SFOest1, SFOest1_p, and SFOest2—against established approaches (PD, CB, PD-WSI, and H-EST). The results demonstrated that SFOest2 consistently outperformed all other methods, achieving the lowest RMSE and BER across varying SNR conditions. Notably, the iterative weight optimization process in SFOest2 effectively refined subcarrier weighting, leading to superior estimation precision and robustness. Meanwhile, SFOest1_p also exhibited competitive performance, benefiting from parameter optimization. The comparative analysis of BER curves further validated the effectiveness of the proposed methods, with SFOest2 achieving the best error performance, followed by SFOest1_p and SFOest1. Overall, our findings highlight the efficacy of the proposed estimation techniques, particularly SFOest2, in mitigating SFO-induced degradation, offering a promising direction for improving OFDM system reliability. Future research could explore machine learning based SFO estimation strategies and hardware implementation for real-world applications.

REFERENCES

[1] Singh, Shivani, et al. "Blind Carrier Frequency Offset Estimation Techniques for Next-Generation Multicarrier Communication Systems: Challenges, Comparative Analysis, and Future Prospects." *IEEE Communications Surveys & Tutorials* (2024).

[2] García, Martín, and Christian Oberli. "Intercarrier interference in OFDM: A general model for transmissions in mobile environments with imperfect synchronization." *EURASIP Journal on Wireless Communications and Networking* 2009 (2009): 1-11.

[3] Wang, Tao, et al. "A Frequency-Domain Estimation Scheme for Frequency Offset with Large Range in OFDM Systems." *Electronics* 14.5 (2025): 859.

[4] Nguyen-Le, Hung, Tho Le-Ngoc, and Chi Chung Ko. "Joint channel estimation and synchronization with inter-carrier interference reduction for OFDM." *2007 IEEE International Conference on Communications*. IEEE, 2007.

[5] Deng, Rui, et al. "SFO compensation by pilot-aided channel estimation for real-time DDO-OFDM system." *Optics Communications* 355 (2015): 172-176.

[6] Wu, Yanan, Rong Mei, and Jie Xu. "Non pilot data-aided carrier and sampling frequency offsets estimation in fast time-varying channel." *Big Data Research* 36 (2024): 100461.

[7] Liu, Yuanhang, et al. "Easy-Hardware-Implementation Algorithm of Carrier and Sampling Frequency Offset Estimation in OFDM Systems." *2024 OES China Ocean Acoustics (COA)*. IEEE, 2024.

[8] Fischer, Volker, and Alexander Kurpiers. "Frequency synchronization strategy for a PC-based DRM receiver." *7th International OFDM-Workshop (InOWo'02), Hamburg*. 2002.

[9] Shim, Eu-Suk, et al. "Synchronization receiver for OFDM-based FM broadcasting systems." *Wireless Personal Communications* 58 (2011): 355-367.

[10] Shin, Won-Jae, Jeongwook Seo, and Young-Hwan You. "MSE analysis of sampling frequency offset estimation scheme for OFDM-based digital radio mondiale (DRM) systems." *Wireless personal communications* 71 (2013): 1271-128.

[11] H. Chuppala, R. Mohan, and R. Shashank, "Sampling clock offset estimation and correction in frequency domain for OFDM receivers," in *TENCON 2017 - 2017 IEEE Region 10 Conference*, IEEE, 2017.

[12] Jung, Yong-An, and Young-Hwan You. "Robust sampling frequency offset estimation for OFDM over frequency selective fading channels." *Applied Sciences* 8.2 (2018): 197.

[13] Liu, Mengyang, et al. "Synchronization Simulation and Analysis of OFDM Wireless Communication Technology." *2019 IEEE 4th International Conference on Computer and Communication Systems (ICCCS)*. IEEE, 2019.

[14] Hsiao, Chien-Yao, et al. "A clock synchronization technique for OFDM-based communications." *2020 IEEE International Conference on Consumer Electronics-Taiwan (ICCE-Taiwan)*. IEEE, 2020.

[15] Kumar, Navin. "Frequency Synchronization in Frequency Domain OFDM-IM based WLAN Systems." *Journal of Communications Software and Systems* 19.3 (2023): 199-206.

[16] Morelli, Michele, and Marco Moretti. "Fine carrier and sampling frequency synchronization in OFDM systems." *IEEE Transactions on Wireless Communications* 9.4 (2010): 1514-1524.

[17] Shi, Kai, Erchin Serpedin, and Philippe Ciblat. "Decision-directed fine synchronization in OFDM systems." *IEEE Transactions on Communications* 53.3 (2005): 408-412.

[18] Garnett, Roman. *Bayesian optimization*. Cambridge University Press, 2023.

[19] Turner, Ryan, et al. "Bayesian optimization is superior to random search for machine learning hyperparameter tuning: Analysis of the black-box optimization challenge 2020." *NeurIPS 2020 Competition and Demonstration Track*. PMLR, 2021.

[20] Lizotte, Daniel James. "Practical bayesian optimization." (2008).

[21] Williams, Christopher KI, and Carl Edward Rasmussen. *Gaussian processes for machine learning*. Vol. 2. No. 3. Cambridge, MA: MIT press, 2006.

[22] Nocedal, Jorge, and Stephen J. Wright, eds. *Numerical optimization*. New York, NY: Springer New York, 1999.

[23] Fletcher, Roger. *Practical methods of optimization*. John Wiley & Sons, 2000.

[24] Robert, Christian P., George Casella, and George Casella. *Monte Carlo statistical methods*. Vol. 2. New York: Springer, 1999.

[25] Dunn, William L., and J. Kenneth Shultis. *Exploring monte carlo methods*. Elsevier, 2022.